This article has been accepted for publication in IEEE Transactions on Magnetics. This is the author's version which has not been fully edited and content may change prior to final publication. Citation information: DOI 10.1109/TMAG.2023.3314835

MSFEM with MOR and DEIM to Solve Nonlinear Eddy Current Problems in Laminated Iron Cores

Karl Hollaus[1], and Markus Schöbinger[1]

[1]Technische Universität Wien, Institute for Analysis and Scientific Computing, A-1040 Vienna, Austria, karl.hollaus@tuwien.ac.at

The computational costs to determine the eddy currents in nonlinear laminated iron cores could be reduced essentially using multiscale finite element methods. However, they are still too high for routine tasks in the design of electrical devices. Therefore, this paper investigates the feasibility of the multiscale finite element method with model order reduction using the discrete empirical interpolation method to facilitate a convenient solution of the nonlinear problem. We propose structure preserving model order reduction to avoid the known large errors due to applying the discrete empirical interpolation method to update the nonlinear right hand side of the fixed point method. Numerical simulations show very satisfactory results.

***Index Terms*—Discrete empirical interpolation method DEIM, iron sheets, model order reduction MOR, multiscale finite element method MSFEM, nonlinear eddy current problems, structural MOR.**

I. Introduction

COMPUTATIONAL costs to compute the eddy currents (ECs) in laminated iron cores can be very high [1]. Our aim is a fast and accurate computation of the ECs in laminated nonlinear iron cores. It turned out that the reduction of the computational costs with the aid of the multiscale finite element method (MSFEM) is not sufficient.

The complexity of a nonlinear eddy current problem (ECP) could be significantly reduced by model order reduction (MOR) in [2]. Proper orthogonal decomposition (POD) is very successful to construct reduced order models for linear problems. However, to assemble the nonlinear term of the finite element (FE) system remains expensive. Therefore, the discrete empirical interpolation method (DEIM) presented in [3] is investigated to substantially improve the efficiency of MOR in the context of MSFEM. MOR with DEIM was successfully applied to a nonlinear static magnetic field problem in [4] and to an ECP in [5].

The algorithm in [3] was used to select the degrees of freedom (DoFs) of the MSFEM for the DEIM. Results of the numerical example in Sec. III demonstrate that MSFEM and MOR with DEIM are capable to provide very accurate results. On the other hand, DEIM is also very sensitive. Very large errors can occur if the dimension of the snapshot matrix for the right hand side (RHS) is too small. A gappy-POD approach was proposed in [5] to eliminate the large errors. Our idea is to apply structure preserving MOR [6], in short structural MOR (SMOR), which exploits the MSFEM approach and has low additional costs.

The simulation results show that MOR and DEIM significantly reduce the memory requirements and computation times of MSFEM, and SMOR is able to significantly minimize the large errors.

II. Numerical Methods

An ECP, such as shown in Fig. 1, is to be solved in the time domain based on the magnetic vector potential (MVP) $\boldsymbol{A}$. The

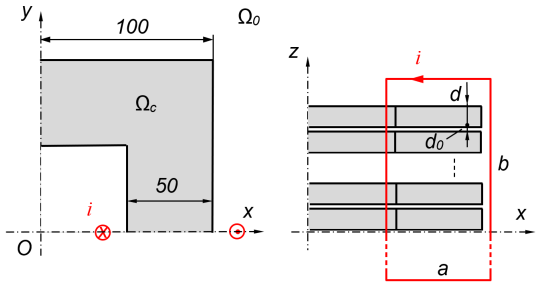

Fig. 1. One eighth of the ECP with 20 iron sheets ($d = 0.5$mm, $d_0 = 0.0125$mm), not drawn to scale, $x = 0$, $y = 0$ and $z = 0$ represent planes of symmetry, dimensions are in mm. Filamentary current loops (red, $f = 50$Hz, $a = 70$mm, $b = 30$mm) are linked with the limbs.

initial boundary value problem reads

$$\begin{aligned} \operatorname{curl}(\nu(\boldsymbol{A})\operatorname{curl}\boldsymbol{A}) + \sigma\frac{\partial}{\partial t}\boldsymbol{A} &= \boldsymbol{J}_0 \quad \text{in } \Omega = \Omega_c \cup \Omega_0 \\ \nu \operatorname{curl}\boldsymbol{A} \times \boldsymbol{n} &= \boldsymbol{0} \quad \text{on } \Gamma_N \\ \boldsymbol{A} \times \boldsymbol{n} &= \boldsymbol{0} \quad \text{on } \Gamma_D, \end{aligned} \tag{1}$$

where ν is the magnetic reluctivity, σ the electric conductivity, $\boldsymbol{J}_0$ a given current density, Ω the domain of the problem consisting of a conducting domain (iron) Ω_c and a non-conducting domain Ω_0 with the boundary $\partial\Omega = \Gamma_N \cup \Gamma_D$.

A. Multiscale Finite Element Method

The 1^{st} order MSFEM approach

$$\tilde{\boldsymbol{A}} = \boldsymbol{A}_0 + \phi_1 \boldsymbol{A}_1 + \operatorname{grad}(\phi_1 w_1) \tag{2}$$

marked by the tilde for the MVP $\boldsymbol{A}$ is used, where $\boldsymbol{A}_0 \in H(\operatorname{curl}, \Omega)$, $\boldsymbol{A}_1 \in H(\operatorname{curl}, \Omega_m)$ and $w_1 \in H^1(\Omega_m)$ are suitably approximated by FE spaces, see [7] and [8], respectively. The micro-shape function ϕ_1 is a periodic, piecewise linear and continuous function [1], i.e. $\phi_1 \in H_{per}(\Omega_m)$. The laminated domain Ω_m consists of iron sheets and insulation layers in between. Essential boundary conditions are prescribed by means of $\boldsymbol{A}_0$ exclusively, and only natural boundary conditions are provided for $\boldsymbol{A}_1$ and w_1. To obtain the weak form of MSFEM,

the approach (2) is inserted into the associated weak form of (1), see e.g. [1].

B. Fixed Point Method

The weak form of the MSFEM of (1) with (2) yields the non-linear ordinary differential equation system

$$A(\nu(\boldsymbol{u}))\boldsymbol{u} + M\frac{\partial}{\partial t}\boldsymbol{u} = \boldsymbol{b}(i) \tag{3}$$

with a nonlinear stiffness matrix $A(\nu)$, a linear mass matrix M, both of dimension $n \times n$, and the filamentary current i in Fig. 1. Applying the fixed point method (FPM) [9] to (3) moves the nonlinear part to the RHS. The Euler method was used as time stepping method (TSM). Thus, (3) becomes

$$\begin{aligned} A(\nu_{FP})\boldsymbol{u}^{(k,l)} + \frac{1}{\Delta t}M\boldsymbol{u}^{(k,l)} = \\ \boldsymbol{b}(i^{(k)}) + A(\nu_{FP} - \nu(\boldsymbol{u}^{(k,l-1)}))\boldsymbol{u}^{(k,l-1)} + \frac{1}{\Delta t}M\boldsymbol{u}^{(k-1)} \end{aligned} \tag{4}$$

with the constant fixed point reluctivity ν_{FP}, the time step Δt, the superscript k for the time instant $t_k = k\Delta t$, which yields $\boldsymbol{u}^{(k)} = \boldsymbol{u}(t_k)$ and the fixed point iteration l. Thus, the nonlinear algebraic equation system (4) has to be solved iteratively at each time instant t_k.

C. Model Order Reduction

To reduce the effort to solve (4), MOR and DEIM are used. A snapshot matrix

$$S = (\boldsymbol{u}^{(1)}, \boldsymbol{u}^{(2)}, ..., \boldsymbol{u}^{(m)}) \tag{5}$$

with m solutions of (4) and simultaneously associated snapshots of the RHS

$$F = (\boldsymbol{f}^{(1)}, \boldsymbol{f}^{(2)}, ..., \boldsymbol{f}^{(m)}) \text{ with } \boldsymbol{f}^{(k)} = \boldsymbol{f}(t_k) \tag{6}$$

are computed. The dimension of S and F equals $n \times m$. Simply selecting S for the projection of (4)

$$S^T\left(A + \frac{1}{\Delta t}M\right)S\boldsymbol{y} = S^T\boldsymbol{f} \tag{7}$$

leads to the reduced order model

$$K\boldsymbol{y} = \boldsymbol{g}, \tag{8}$$

where $K \in \mathbb{R}^{m\times m}$ with $m \ll n$. The reduced system (8) maintains the nonlinearity of the original large system (3).
A POD based on the singular value decomposition (SVD) is too expensive for large problems and therefore avoided. The application of the Gram-Schmidt orthogonalization method to (5) of the numerical problem in Sec. III did not help at all. If the dimension of the matrix S would be too small, an adaptive MOR could be considered. This has not been applied in the present work.
The most expensive part to solve (8) is to update the nonlinear RHS. To cope with this burden DEIM is investigated for MSFEM.

D. Discrete Empirical Interpolation Method

The matrix F is used to enable a fast update of $\boldsymbol{f}$. For feasibility of the DEIM the approximation

$$F\boldsymbol{c} \approx \boldsymbol{f} \tag{9}$$

should hold for any RHS $\boldsymbol{f}$ as good as possible. Since (9) is strongly overdetermined, the algorithm in [3] was chosen in order to still determine a unique vector $\boldsymbol{c}$. Simply speaking, the algorithm recursively searches for m dominant entries in the column vectors of F resulting in a regular matrix G of dimension $m \times m$. Thus, only the m entries of $\boldsymbol{f}$ corresponding to the previous search really have to be determined and the nonlinear $\nu(\boldsymbol{A})$ of the associated FEs updated. Then, $\boldsymbol{c}$ can be uniquely calculated with G. The remaining entries of $\boldsymbol{f}$ are obtained inexpensively by means of (9) with the known $\boldsymbol{c}$. For a more detailed explanation we refer to [3].

E. Structural Model Order Reduction

The idea is to enlarge the space spanned by a given snapshot matrix F without computing more snapshots $\boldsymbol{f}_i$, which would be expensive. Therefore SMOR has been applied such that a RHS vector

$$\boldsymbol{f} = (\boldsymbol{f}_{\boldsymbol{A}_0}, \boldsymbol{f}_{\boldsymbol{A}_1}, \boldsymbol{f}_{w_1})^T \tag{10}$$

is decomposed according to the unknown variables $\boldsymbol{A}_0$, $\boldsymbol{A}_1$ and w_1 in the MSFEM approach (2) and consequently F can be written as

$$F = (F_{\boldsymbol{A}_0}, F_{\boldsymbol{A}_1}, F_{w_1})^T, \tag{11}$$

where T means transposed. Using SMOR leads to the approximation

$$(F_{\boldsymbol{A}_0}\boldsymbol{c}_{\boldsymbol{A}_0}, F_{\boldsymbol{A}_1}\boldsymbol{c}_{\boldsymbol{A}_1}, F_{w_1}\boldsymbol{c}_{w_1})^T \approx \boldsymbol{f} \tag{12}$$

with the unknown vectors $\boldsymbol{c}_{\boldsymbol{A}_0}$, $\boldsymbol{c}_{\boldsymbol{A}_1}$ and $\boldsymbol{c}_{w_1}$, respectively, which are uniquely determined with the decompositions (10) and (11) and using (12) analog to $\boldsymbol{c}$ in (9) with the algorithm in [3]. Projection of (12) based on the decomposition of SMOR results in

$$\boldsymbol{g} = (\boldsymbol{g}_{\boldsymbol{A}_0}, \boldsymbol{g}_{\boldsymbol{A}_1}, \boldsymbol{q}_{w_1})^T, \tag{13}$$

where

$$\begin{aligned} \boldsymbol{g}_{\boldsymbol{A}_0} &= S^T(F_{\boldsymbol{A}_0}\boldsymbol{c}_{\boldsymbol{A}_0}, \boldsymbol{0}, \boldsymbol{0})^T, \\ \boldsymbol{g}_{\boldsymbol{A}_1} &= S^T(\boldsymbol{0}, F_{\boldsymbol{A}_1}\boldsymbol{c}_{\boldsymbol{A}_1}, \boldsymbol{0})^T, \\ \boldsymbol{g}_{w_1} &= S^T(\boldsymbol{0}, \boldsymbol{0}, F_{w_1}\boldsymbol{c}_{w_1})^T. \end{aligned} \tag{14}$$

III. Numerical Simulations and Results

The numerical example with details is presented in Fig. 1. The used magnetization curve can be found in [1]. A conductivity of $\sigma = 2 \cdot 10^6$S/m was selected. The nonlinear iterations l were stopped as soon as the criterion

$$\varepsilon = \frac{\|\boldsymbol{u}^{(l)}(t_k) - \boldsymbol{u}^{(l-1)}(t_k)\|}{\|\boldsymbol{u}^{(l)}(t_k)\|} < 10^{-3} \tag{15}$$

was met. This criterion was also used with the DEIM. To evaluate the feasibility of MSFEM and MOR with DEIM, the time behavior of the EC losses

$$p(t) = \int_{\Omega_c} \sigma\frac{\partial}{\partial t}\boldsymbol{A} \cdot \frac{\partial}{\partial t}\boldsymbol{A}\, d\Omega \tag{16}$$

was studied.

This article has been accepted for publication in IEEE Transactions on Magnetics. This is the author's version which has not been fully edited and content may change prior to final publication. Citation information: DOI 10.1109/TMAG.2023.3314835

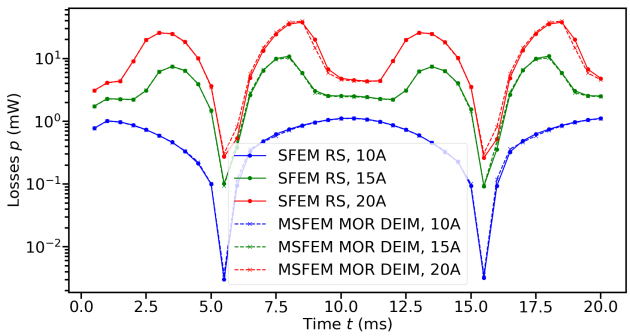

Fig. 2. Losses obtained by SFEM and MSFEM using MOR with DEIM for different excitations $\hat{\imath}$ in A.

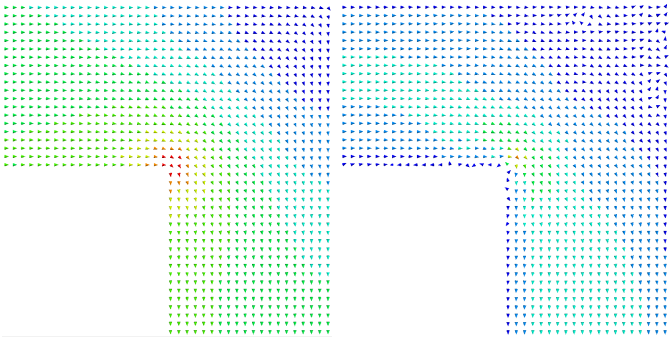

Fig. 3. Magnetic flux density $\boldsymbol{B}$ with $\hat{\imath}$=20A at t=15.0ms, MSFEM (left, scaling: $0 < \boldsymbol{B} < 1.0$T), difference between MSFEM and MSFEM with MOR and DEIM (right, scaling: $0 < |\boldsymbol{B}| < 0.01$T).

A. Losses and Fields

The first 10 solutions from the TSM with $\Delta t = 0.5ms$ were selected as snapshots S as well as the corresponding RHS vectors for F.

EC losses obtained by the standard FEM (SFEM) served as a reference solution (RS). A comparison with those obtained by MSFEM and MOR with DEIM are shown in Fig. 2. The agreement of the losses is very satisfactory. The influence of the magnetization curve is clearly visible. There is also a satisfactory agreement of the magnetic flux density $\boldsymbol{B}$ obtained by MSFEM and MOR with DEIM compared with MSFEM only as shown in Fig. 3. The same holds for the current density $\boldsymbol{J}$, see Fig. 4.

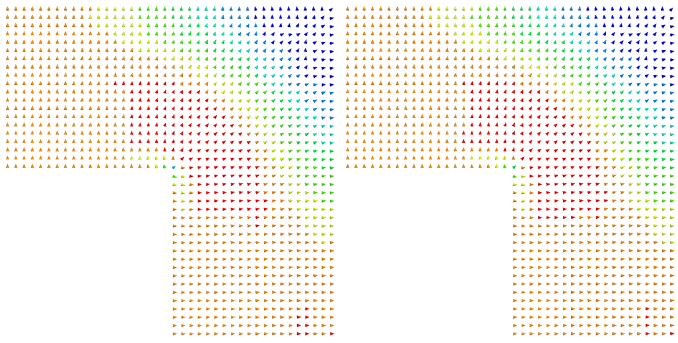

Fig. 4. Current density $\boldsymbol{J}$ with $\hat{\imath}$=20A at t=15.0ms, scaling: $-1 \cdot 10^3 < |\boldsymbol{J}| < 2 \cdot 10^4$A/m, MSFEM (left) and with MOR and DEIM (right).

TABLE I
NO. OF DEGREES OF FREEDOM.

Method(s)	SFEM	MSFEM	MSFEM and MOR
DoFs	1 116,860	103,879	6, 8 or 10

TABLE II
COMPUTATION TIME IN S.

$\hat{\imath}$ in A	MSFEM [1])	MOR with DEIM [2])
5	606	518
10	514	319
15	603	523
20	636	535

[1]) for a quarter period, [2]) for the whole period, $\varepsilon < 10^{-4}$ for $\hat{\imath} = 5$A

B. Computational Costs

The required number of DoFs are summarized in Tab. I. It shows clearly the reduction of the size of the system of equations to be solved. The computation time of MSFEM and MOR with DEIM is less than a quarter of MSFEM only as shown in Tab. II. The parameter ε in (15) had to be set to 10^{-4} for $\hat{\imath} = 5$A to obtained a sufficiently accurate solution. The FPM required a moderate number of iterations as can be seen in Fig. 5 to solve the nonlinear problem (4).

C. Visualisation of DEIM DoFs

To fix the locus of a DoF in space the center of gravity

$$\boldsymbol{r}_c = \frac{\int_\Omega \|v\|_{L_2} \boldsymbol{r}\, d\Omega}{\int_\Omega \|v\|_{L_2}\, d\Omega}, \text{ where } \boldsymbol{r} = (x, y, z)^T, \qquad (17)$$

of the respective basis function v was computed. The loci of the DEIM DoFs are shown in Fig. 7. The single DoF 2 in air belongs to $\boldsymbol{A}_0$, all other DoFs to $\boldsymbol{A}_1$. DoFs of w_1 seem not to be relevant for the used algorithm and given problem.

The distribution of the DEIM DoFs to the components of (2) remains the same for all excitations $\hat{\imath}$ as shown in Tab. III. The affected DEIM DoFs of $\boldsymbol{A}_1$ vary with the excitation $\hat{\imath}$. The DEIM patches in terms of the required number of FEs and DoFs in order to update the material for the DEIM DoFs can be found in Tab. III, compare also with Fig. 6. The number of FEs for the DEIM-DoFs is different depending on whether the FEs are on the boundary of Ω_m or not.

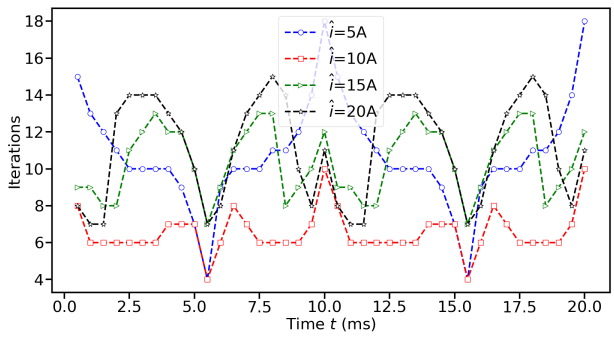

Fig. 5. Required nonlinear iterations for the FPM, $m = 10$ and $\Delta t = 0.5$ms, different excitations $\hat{\imath}$ in A, $\varepsilon < 10^{-4}$ for $\hat{\imath} = 5$A.

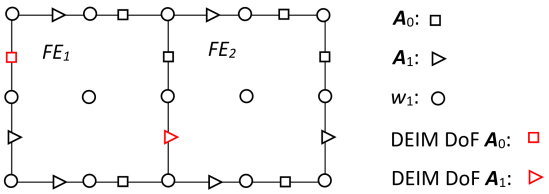

Fig. 6. Sketch of a FE DEIM patch with the FEs FE_1 and FE_2. The DEIM DoFs belong to an $\boldsymbol{A}_0$- and an $\boldsymbol{A}_1$-component of the MSFEM approach (2).

TABLE III
NO. DEIM DOFS AND SIZE OF DEIM DOF PATCHES.

$\hat{i}$ in A	$\boldsymbol{A}_0$	$\boldsymbol{A}_1$	w_1	FEs	DoFs
5	1	9	0	22	1948
10	1	9	0	30	2824
15	1	9	0	36	3476
20	1	9	0	32	3120

$\varepsilon < 10^{-4}$ for $\hat{i} = 5\mathrm{A}$

D. Snapshots and SMOR

The choice of snapshots is examined in Fig. 8. The poor results show how critical the choice of m snapshots is in F. The pronounced large errors occur with only 6 snapshots at $\hat{i}$=10A. The reason is a too small dimension of F. The large errors are significantly minimized by SMOR with 6 snapshots, as shown in Fig. 9. However, SMOR also exhibits a slightly larger error for a higher number of snapshots in F.

CONCLUSIONS

The large reduction in computational cost and the very good results demonstrate the usefulness of MSFEM and MOR with DEIM. The sensitivity of DEIM with respect to the number of snapshots in the RHS matrix F can be significantly minimized with SMOR at negligible additional cost. However, the field distributions obtained with SMOR show a larger error than those obtained with MOR shown in Figs. 3 and 4).

ACKNOWLEDGMENT

This work was supported by the Austrian Science Fund (FWF) under projects P 31926.

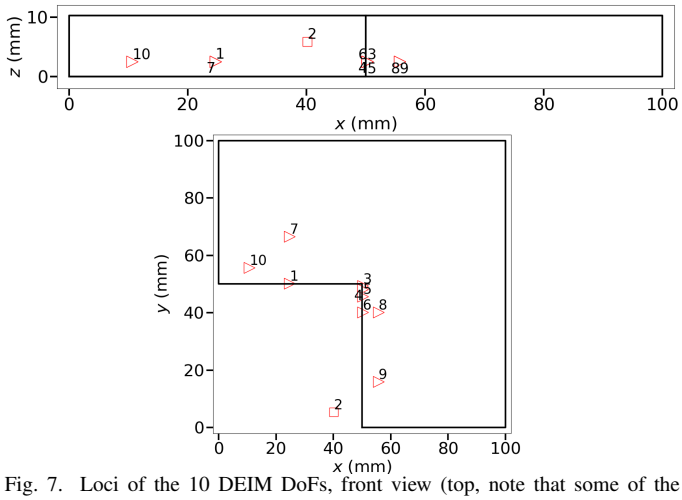

Fig. 7. Loci of the 10 DEIM DoFs, front view (top, note that some of the DoFs are hidden by others), top view (bottom). See legend in Fig. 6.

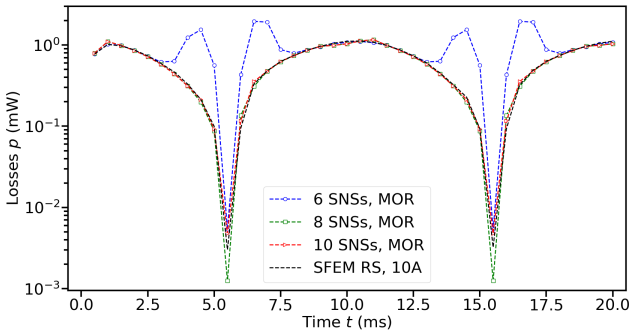

Fig. 8. Losses obtained by MSFEM using MOR with DEIM for different numbers m of snapshots S, $\Delta t = 0.5\mathrm{ms}$, $\hat{i}$=10A.

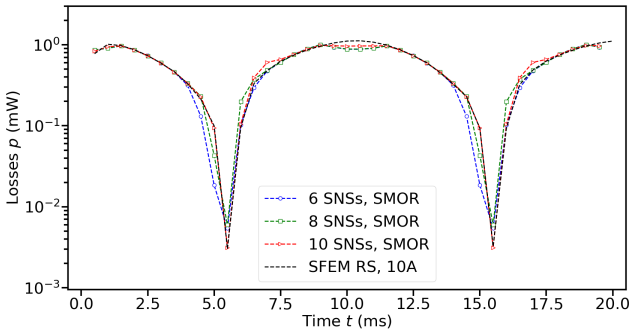

Fig. 9. Losses obtained by MSFEM using SMOR with DEIM for different numbers m of snapshots S, $\Delta t = 0.5\mathrm{ms}$, $\hat{i}$=10A.

REFERENCES

[1] K. Hollaus, "A MSFEM to Simulate the Eddy Current Problem in Laminated Iron Cores in 3D," *COMPEL*, vol. 38, no. 5, pp. 1667–1682, 2019.

[2] K. Hollaus, J. Schöberl, and M. Schöbinger, "MSFEM and MOR to Minimize the Computational Costs of Nonlinear Eddy-Current Problems in Laminated Iron Cores," *IEEE Trans. Magn.*, vol. 56, no. 2, pp. 1–4, Feb 2020.

[3] S. Chaturantabut and D. C. Sorensen, "Nonlinear model reduction via discrete empirical interpolation," *SIAM Journal on Scientific Computing*, vol. 32, no. 5, pp. 2737–2764, 2010.

[4] T. Henneron and S. Clénet, "Model Order Reduction of Non-Linear Magnetostatic Problems Based on POD and DEI Methods," *IEEE Trans. Magn.*, vol. 50, no. 2, pp. 33–36, Feb 2014.

[5] M. R. Hasan, L. Montier, T. Henneron, and R. V. Sabariego, "Stabilized Reduced-Order Model of a Non-Linear Eddy Current Problem by a Gappy-POD Approach," *IEEE Transactions on Magnetics*, vol. 54, no. 12, pp. 1–8, 2018.

[6] L. Montier, A. Pierquin, T. Henneron, and S. Clénet, "Structure Preserving Model Reduction of Low-Frequency Electromagnetic Problem Based on POD and DEIM," *IEEE Trans. Magn.*, vol. 53, no. 6, pp. 1–4, June 2017.

[7] J. Schöberl and S. Zaglmayr, "High order Nédélec elements with local complete sequence properties," *COMPEL*, vol. 24, no. 2, pp. 374–384, 2005.

[8] K. Hollaus and J. Schöberl, "Some 2-D Multiscale Finite-Element Formulations for the Eddy Current Problem in Iron Laminates," *IEEE Trans. Magn.*, vol. 54, no. 4, pp. 1–16, April 2018.

[9] M. Chiampi, D. Chiarabaglio, and M. Repetto, "A Jiles-Atherton and fixed-point combined technique for time periodic magnetic field problems with hysteresis," *IEEE Transactions on Magnetics*, vol. 31, no. 6, pp. 4306–4311, 1995.